Evaluation of Special Structural Wall System with Belt Truss and Outrigger on Supertall Building in Jakarta

Muhamad Cesar Vitho[1*], Budi Kudwadi[1] and Ben Novarro Batubara[1]
Civil Engineering Study Program, Indonesia University of Education
*Corresponding Author: Muhamad Cesar Vitho. Email: mcesarvitho@upi.edu

Abstract

The construction of supertall buildings in Jakarta addresses land scarcity and demand for vertical space. Their extreme height creates challenges in resisting earthquake forces, requiring efficient structural systems. This study evaluates the effectiveness of belt truss and outrigger systems in reducing displacement and drift, with performance assessed by ATC-40. Earthquake loading was analyzed using the response spectrum method in ETABS 2020 with three models. Model 1 applied the system at floors 35–36 and 55–57, Model 2 excluded the system, and Model 3 placed it at floors 18–20, 37–39, and 56–57. The evaluation focused on the 78th floor. Model 1 showed displacement of 329.195 mm in X and 342.202 mm in Y, with drift of 31.224 mm in X and 33.076 mm in Y. Model 2 produced the largest displacement 331.526 mm in X and 347.076 mm in Y, with drift of 31.620 mm in X and 33.698 mm in Y. Model 3 performed best, with displacement of 324.286 mm in X and 336.759 mm in Y, and drift of 31.086 mm in X and 32.495 mm in Y. All models reached Immediate Occupancy, showing the structure remains functional after an earthquake. These results confirm that belt truss and outrigger systems enhance stiffness and reduce deformation, making them essential for supertall buildings in seismic-prone regions.

Keywords: Supertall building, belt truss, outrigger, response spectrum, displacement, inter-story drift, ATC-40

1. INTRODUCTION

The growth of high-rise building construction in urban areas such as Jakarta continues to show significant increases in response to limited horizontal land and the growing need for vertical space for residential, office, and other commercial functions. This phenomenon reflects a strategic push toward maximizing the use of vertical space to support the economic and social activities of urban communities. However, the increase in building height is accompanied by more complex technical challenges, particularly regarding stability against lateral forces such as earthquakes and wind. In earthquake-prone areas like Jakarta, the structural design of high-rise buildings must meet strict earthquake resistance standards to ensure the safety and comfort of occupants. To address these challenges, one structural approach deemed effective is the application of belt truss and outrigger systems combined with vertical core elements such as corewalls. This system efficiently distributes lateral forces, enhances structural stiffness, and reduces inter-story drift, enabling buildings to function optimally post-earthquake.

As one of the most widely applied earthquake-resistant structural systems in modern high-rise buildings, the combination of belt trusses and outriggers has proven effective in enhancing lateral stability and maintaining structural performance under extreme conditions. This system leverages the interaction between internal and external structural elements through rigid connecting components, creating an effective collaborative system in responding to deformations caused by earthquake loads. Evaluating the effectiveness of this system is crucial, especially for extremely tall buildings (supertall buildings) that face a higher risk of structural failure. Therefore, this study aims to analyze how effectively the belt truss and outrigger system can reduce lateral displacement and interstory drift through a numerical analysis approach based on the response spectrum method. Additionally, this study evaluates structural performance based on the performance-based design approach outlined in ATC-40, with the aim of providing qualitative and quantitative insights into the safety level and post-earthquake functionality of the structure. The findings from this study are expected to contribute to the development of technical references and practical considerations in the design of tall buildings in earthquake-prone areas.

2. METHOD

This research was conducted using earthquake loading with the response spectrum method, followed by numerical analysis to evaluate the effectiveness of the belt truss and outrigger systems in controlling lateral deformation in supertall buildings subjected to earthquake loads. Structural modeling was performed in three dimensions using ETABS 2020 software with a simplified structural system configuration in accordance with the scope of the academic study. The response spectrum method was chosen because it can efficiently represent the dynamic response of a building to earthquake excitation and is consistent with the linear elastic approach commonly used in the design of tall buildings. The evaluation was conducted on structural responses in the form of inter-story

drifts and displacements, with structural performance assessed based on criteria from ATC-40. All earthquake loading parameters refer to the provisions of SNI 1726:2019 to ensure compliance with national standards for earthquake-resistant structural design. Three scenarios were analyzed: model 1 with the existing system on floors 35 to 36 and 55 to 57, model 2 without the system, and model 3 with the system on floors 18 to 20, 37 to 39, and 56 to 57.

2.1. Structural Models

For the purpose of evaluating the effectiveness of the belt truss and outrigger systems, three structural models were developed with uniform geometric configurations and loading conditions, with the main difference being the variation in the placement of the lateral force restraint systems. The modeling was carried out by maintaining consistency in the main structural elements across all three models, such as beams, columns, composite columns, core walls, floor slabs, as well as the belt truss and outrigger systems. The technical specifications for the structural elements of the belt truss and outrigger systems used are summarized as follows:

Table 1: Structural Element Properties of Belt Truss and Outriggers Model 1

No.	Story	H Beam (mm)
1	L35-36	700X700X70X80 (Outrigger) 600X600X40X50 (Belt Truss)
2	L55-57	

Table 2: Structural Element Properties of Belt Truss and Outriggers Model 3

No.	Story	H Beam (mm)
1	L18-20	700X700X70X80 (Outrigger) 600X600X40X50 (Belt Truss)
2	L37-39	
3	L56-57	

The following is a floor plan of a supertall building modeled with 3D visualization displayed by ETABS software based on the above property data.

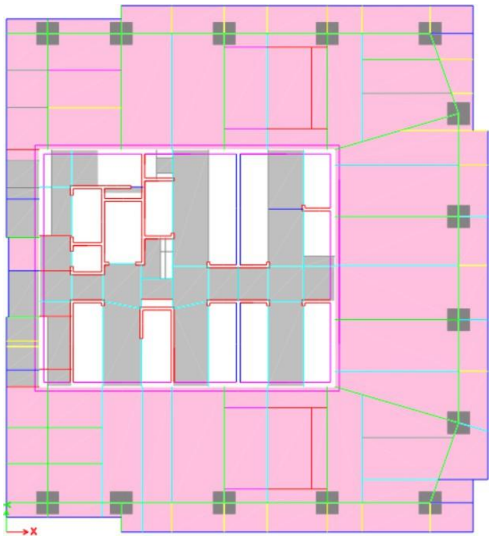

Figure 1. Typical Floor Plan for Floors 1-40 Models 1, 2, and 3

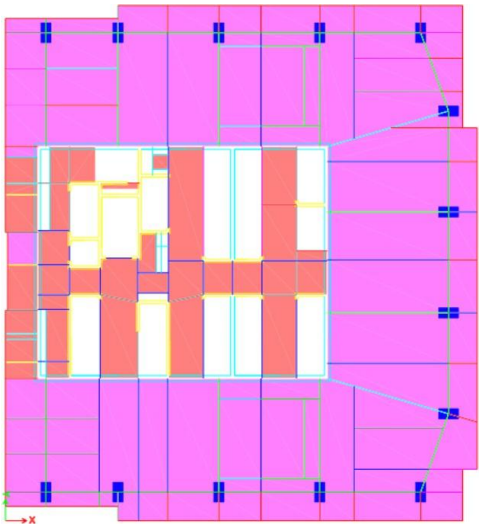

Figure 2. Typical Floor Plan for Floors 41-Roof Models 1, 2, and 3

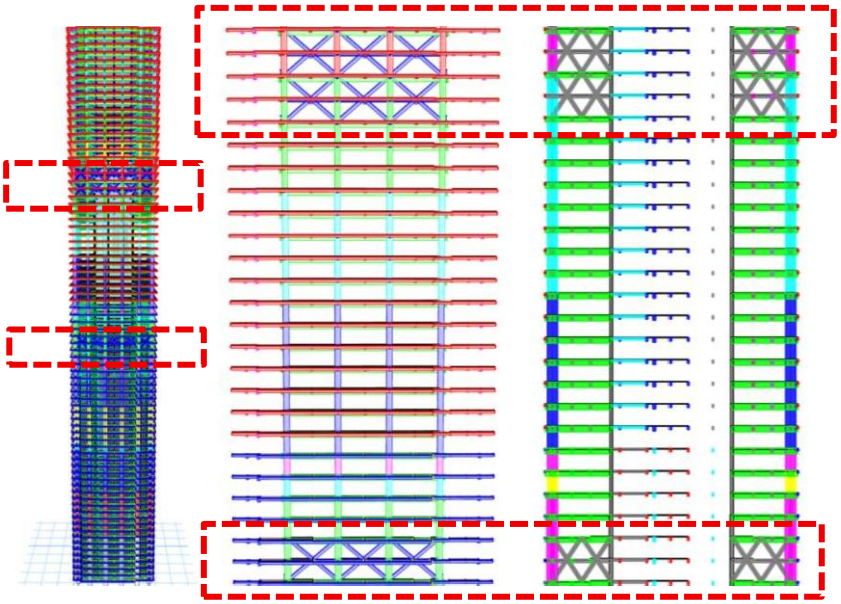

Figure 3. 3D Visual and Appearance of The Belt Truss and Outrigger Structure of Model 1

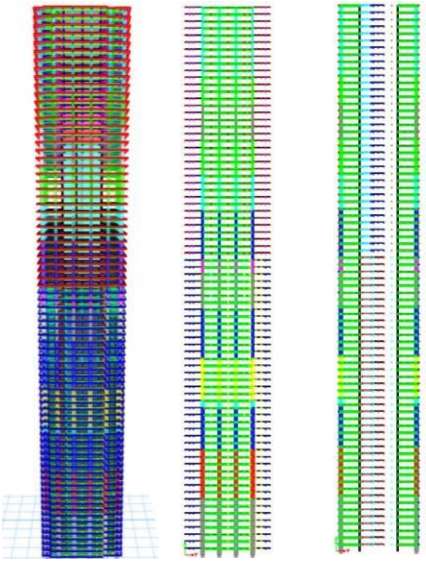

Figure 4. 3D Visual Model 2 and Appereance Without Belt Truss and Outrigger Structure of Model 2

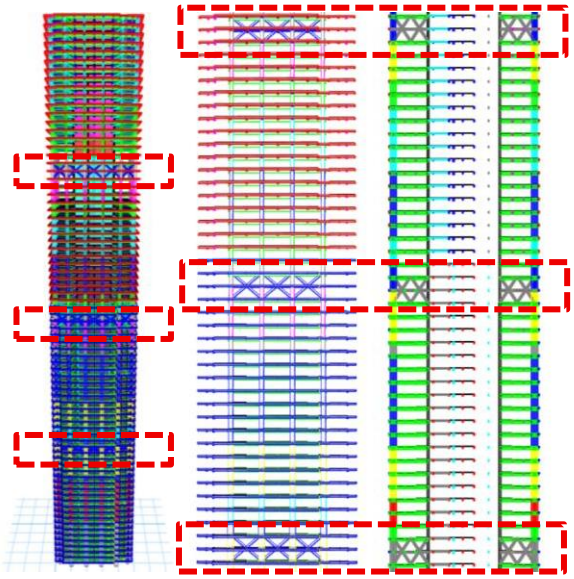

Figure 5. 3D Visual and Appearance of The Belt Truss and Outrigger Structure of Model 3

2.2. Load Calculation

Dead load in supertall buildings is the load that comes from the weight of the building's structural elements themselves, such as the weight of columns, beams, slabs, core walls, belt trusses, and outriggers. To calculate this weight, ETABS software can automatically calculate the weight of each structural element by inputting the specific weight of each structural element and then defining it as 1 in the load case. In addition to dead load, there is also additional dead load, often abbreviated as SIDL. SIDL is a permanent load caused by non-structural elements, which are often caused by building finishing components. In inputting additional dead load on supertall buildings, there are several components defined as follows.

Table 3: Super Imposed Dead Load

SIDL			
	Component	**Load**	
		kg/m²	**kN/m²**
Floor Slab	2 cm Spesi	42	0.412
	0.5 cm Ceramic	12	0.118
	Ceiling	11	0.108
	Ceiling Hanger	7	0.069
	MEP	25	0.245
	Total	**97**	**0.951**
Roof Slab	0.5 cm Asphalt	7	0.069
	Ceiling	11	0.108
	Ceiling Hanger	7	0.069
	MEP	25	0.245
	Total	**50**	**0.490**

Based on SNI 1727-2020, which specifies the minimum design loads for buildings, the live loads for the supertall building fall into the category of evenly distributed live loads for office spaces and live loads for roofs that are not used for residential purposes. The following are the live loads used in the load calculation.

Table 4: Load Live

Load Live		
Component	**Load**	
	kg/m²	**kN/m²**
Floor Slab	240	2.354
Roof Slab	96	0.941

In calculating the seismic load that will be received by the supertall building structure modeling, several design parameter data are required based on SNI 1726-2019 regulations on procedures for planning seismic resistance for building structures. The following are the design parameters obtained.

Table 5: Earthquake Design Parameters

Risk Category	II (Office Building)
Earthquake Importance Factor (Ie)	1.0
Site Classification	SD (Medium Soil)
Seismic Design Category	D
Response Modification Coefficient (R)	7
System Strength Factor (Ω_0)	2.5
Deflection Amplification Factor (Cd)	5.5

Then, to obtain the short-period spectral acceleration (S_s) and 1-second spectral acceleration (S_1) values, we searched for areas in Jakarta with moderate soil classification (SD) as follows.

$S_s = 0.7806$ g

$S_1 = 0.3823$ g

Based on the S_s value and the S_1 value, the short period site coefficient (F_a) and the 1-second period site coefficient (F_v) are obtained as follows.

$F_a = 1.1878$

$F_v = 1.9177$

Thus, the acceleration spectral response parameters for short periods (S_{MS}) and acceleration spectral response parameters for 1-second periods (S_{M1}) were also obtained.

$S_{MS} = 0.9272$ g

$S_{M1} = 0.7331$ g

After that, obtain the design spectral acceleration parameter values for short periods (S_{DS}) and the design spectral acceleration parameters for 1-second periods (S_{D1}).

$S_{DS} = 0.6181$ g

$S_{D1} = 0.4888$ g

Finally, the following design response spectrum was obtained.

$T_0 = 0.1581$ detik

$T_s = 0.7907$ detik

$T_L = 20$ detik

The following are the design acceleration response period and spectrum.

Table 6: Design Accelaration Response Period and Spectrum

T (second)	Sa (g)	T (second)	Sa (g)
0	0.2472	12	0.0407
0.1581	0.6181	13	0.0376
0.7907	0.6181	14	0.0349
1	0.4888	15	0.0326
2	0.2444	16	0.0305
3	0.1629	17	0.0288
4	0.1222	18	0.0272
5	0.0978	19	0.0257
6	0.0815	20	0.0244
7	0.0698	21	0.0222
8	0.0611	22	0.0202
9	0.0543	23	0.0185
10	0.0489	24	0.0170
11	0.0444	25	0.0156

The following is the design acceleration response spectrum curve.

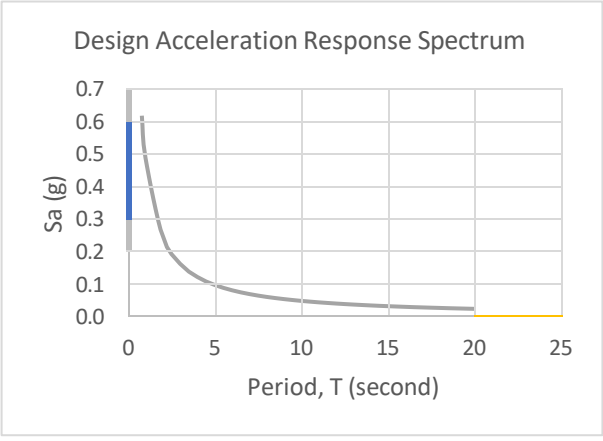

Figure 6. Design Acceleration Response Spectrum Curve.

The following data will be used for calculating the fundamental period of the approach.

$C_u = 1.4$

$C_t = 0.0488$

$x = 0.75$

$h_n = 347.1$ m

The following are the results and calculations of the fundamental approach period (T_a), maximum period (T_{max}), and analysis period (T_c) for each modeling.

$T_a = 3.924$ second

$T_{max} = 5.494$ second

After obtaining the seismic response coefficient calculation results, the seismic base shear force value can be calculated for each model and then a new factor is scaled to equalize the static base shear force and dynamic base shear force values.

3. RESULTS AND DIDCUSSION

Based on SNI 1726-2019 regulations, which state that the deviation between design levels (Δ) must not exceed the deviation between permit levels (Δa), supertall buildings are classified as structures with risk category II because they function as office buildings and have a formula for the limit of deviation between permit levels (Δa) equal to 0.020hsx, where hsx is the height of the level below the x-level location. In calculating the deviation between levels, the displacement output values from each model analyzed by the ETABS software are required. The following is the formula for calculating drift.

$$\Delta = (Cd \times \Delta e) / Ie \quad (1)$$

Table 7: Displacement and Drift Values in Model 1

Story	Displacement		Elastic Drift		h_{sx}	Inelastic Drift		Drift Limit	Control
	δe_X	δe_Y	δe_X	δe_Y		Δ_X	Δ_Y	Δa	
	(mm)	(mm)	(mm)	(mm)	(mm)	(mm)	(mm)	(mm)	
78	329.195	370.284	5.677	6.423	4450	31.224	35.327	89.000	OK
77	323.518	363.861	5.691	6.109	4450	31.300	33.599	89.000	OK
76	317.827	357.752	5.697	6.114	4450	31.334	33.627	89.000	OK
75	312.130	351.638	5.700	6.119	4450	31.350	33.654	89.000	OK
74	306.430	345.519	5.702	6.123	4450	31.361	33.676	89.000	OK
73	300.728	339.396	5.701	6.122	4450	31.356	33.671	89.000	OK
72	295.027	333.274	5.700	6.121	4450	31.350	33.665	89.000	OK
71	289.327	327.153	5.694	6.113	4450	31.317	33.622	89.000	OK
70	283.633	321.040	5.686	6.103	4450	31.273	33.567	89.000	OK
69	277.947	314.937	5.677	6.082	4450	31.224	33.451	89.000	OK
68	272.270	308.855	5.661	6.055	4450	31.136	33.303	89.000	OK
67	266.609	302.800	5.645	6.044	4450	31.047	33.242	89.000	OK
66	260.964	296.756	5.625	6.014	4450	30.938	33.077	89.000	OK
65	255.339	290.742	5.604	5.968	4450	30.822	32.824	89.000	OK
64	249.735	284.774	5.569	5.913	4450	30.630	32.522	89.000	OK
63	244.166	278.861	5.541	5.912	4450	30.476	32.516	89.000	OK
62	238.625	272.949	5.481	5.844	4450	30.146	32.142	89.000	OK
61	233.144	267.105	5.314	5.638	4450	29.227	31.009	89.000	OK
60	227.830	261.467	5.287	5.447	4450	29.079	29.959	89.000	OK
59	222.543	256.020	5.251	5.553	4450	28.881	30.541	89.000	OK
58	217.292	250.467	5.252	5.429	4450	28.886	29.860	89.000	OK
57	212.040	245.038	5.365	5.725	4450	29.507	31.488	89.000	OK
56	206.675	239.313	5.363	5.777	4450	29.497	31.773	89.000	OK
55	201.312	233.536	5.344	5.786	4450	29.392	31.823	89.000	OK
54	195.968	227.750	5.319	5.790	4450	29.254	31.845	89.000	OK
53	190.649	221.960	5.294	5.792	4450	29.117	31.856	89.000	OK
52	185.355	216.168	5.264	5.785	4450	28.952	31.818	89.000	OK
51	180.091	210.383	5.232	5.771	4450	28.776	31.741	89.000	OK
50	174.859	204.612	5.198	5.750	4450	28.589	31.625	89.000	OK
49	169.661	198.862	5.161	5.725	4450	28.386	31.488	89.000	OK
48	164.500	193.137	5.123	5.701	4450	28.176	31.356	89.000	OK
47	159.377	187.436	5.081	5.666	4450	27.946	31.163	89.000	OK
46	154.296	181.770	5.039	5.628	4450	27.714	30.954	89.000	OK
45	149.257	176.142	4.992	5.585	4450	27.456	30.718	89.000	OK
44	144.265	170.557	4.945	5.535	4450	27.198	30.443	89.000	OK
43	139.320	165.022	4.889	5.476	4450	26.889	30.118	89.000	OK
42	134.431	159.546	4.834	5.409	4450	26.587	29.750	89.000	OK
41	129.597	154.137	4.779	5.337	4450	26.285	29.353	89.000	OK
40	124.818	148.800	4.718	5.286	4450	25.949	29.073	89.000	OK
39	120.100	143.514	4.626	5.185	4450	25.443	28.518	89.000	OK
38	115.474	138.329	4.409	4.827	4450	24.250	26.549	89.000	OK
37	111.065	133.502	4.362	4.693	4450	23.991	25.812	89.000	OK
36	106.703	128.809	4.478	5.018	4450	24.629	27.599	89.000	OK
35	102.225	123.791	4.449	5.041	4450	24.470	27.726	89.000	OK
34	97.776	118.750	4.405	5.036	4450	24.228	27.698	89.000	OK
33	93.371	113.714	4.356	5.013	4450	23.958	27.572	89.000	OK
32	89.015	108.701	4.303	4.982	4450	23.667	27.401	89.000	OK
31	84.712	103.719	4.247	4.945	4450	23.359	27.198	89.000	OK
30	80.465	98.774	4.187	4.902	4450	23.029	26.961	89.000	OK
29	76.278	93.872	4.124	4.849	4450	22.682	26.670	89.000	OK
28	72.154	89.023	4.057	4.791	4450	22.314	26.351	89.000	OK

Story	Displacement		Elastic Drift		h_{sx}	Inelastic Drift		Drift Limit	Control
	δe_X	δe_Y	δe_X	δe_Y		Δ_X	Δ_Y	Δa	
	(mm)	(mm)	(mm)	(mm)	(mm)	(mm)	(mm)	(mm)	
27	68.097	84.232	3.987	4.740	4450	21.929	26.070	89.000	OK
26	64.110	79.492	3.913	4.674	4450	21.522	25.707	89.000	OK
25	60.197	74.818	3.836	4.602	4450	21.098	25.311	89.000	OK
24	56.361	70.216	3.753	4.522	4450	20.642	24.871	89.000	OK
23	52.608	65.694	3.668	4.430	4450	20.174	24.365	89.000	OK
22	48.940	61.264	3.573	4.333	4450	19.652	23.832	89.000	OK
21	45.367	56.931	3.469	4.235	4450	19.080	23.293	89.000	OK
20	41.898	52.696	3.367	4.138	4450	18.519	22.759	89.000	OK
19	38.531	48.558	3.239	4.003	4450	17.815	22.017	89.000	OK
18	35.292	44.555	3.138	3.882	4450	17.259	21.351	89.000	OK
17	32.154	40.673	3.035	3.769	4450	16.693	20.730	89.000	OK
16	29.119	36.904	2.925	3.643	4450	16.088	20.037	89.000	OK
15	26.194	33.261	2.809	3.511	4450	15.450	19.311	89.000	OK
14	23.385	29.750	2.687	3.378	4450	14.779	18.579	89.000	OK
13	20.698	26.372	2.546	3.218	4450	14.003	17.699	89.000	OK
12	18.152	23.154	2.416	3.061	4450	13.288	16.836	89.000	OK
11	15.736	20.093	2.280	2.898	4450	12.540	15.939	89.000	OK
10	13.456	17.195	2.135	2.725	4450	11.743	14.988	89.000	OK
9	11.321	14.470	1.983	2.535	4450	10.907	13.943	89.000	OK
8	9.338	11.935	1.820	2.335	4450	10.010	12.843	89.000	OK
7	7.518	9.600	1.642	2.119	4450	9.031	11.655	89.000	OK
6	5.876	7.481	1.472	1.899	4450	8.096	10.445	89.000	OK
5	4.404	5.582	1.293	1.668	4450	7.112	9.174	89.000	OK
4	3.111	3.914	1.106	1.419	4450	6.083	7.805	89.000	OK
3	2.005	2.495	0.907	1.152	4450	4.989	6.336	89.000	OK
2	1.098	1.343	0.696	0.866	4450	3.828	4.763	89.000	OK
1	0.402	0.477	0.402	0.477	4450	2.211	2.624	89.000	OK

Based on the output results from ETABS in modeling 1, the maximum displacement value on floor 78 was obtained at 329.195 mm in the X direction and 370.284 mm in the Y direction. Therefore, the calculation of the inter-story drift in modeling 1 with the placement of the existing belt truss and outrigger system obtained a maximum drift value on floor 78 (top story) caused by the seismic response spectrum in the X direction of 31.224 mm and in the Y direction of 35.327 mm.

Based on the above results, it can be seen that in the first model, where the belt truss and outrigger systems were placed at floor heights 35–36 and 55–57 in accordance with the actual configuration, the maximum displacement recorded was 329.195 mm in the X direction and 370.284 mm in the Y direction. These results directly reflect that the application of the belt truss and outrigger system, limited to only two vertical levels, does contribute positively to enhancing lateral stiffness; however, it is not yet sufficiently optimal in reducing the total structural displacement comprehensively. This is due to the uneven distribution of lateral stiffness along the building's height, causing lateral forces from seismic loads to still induce significant deformation, particularly in the upper areas of the structure. In other words, while the presence of the system is proven to be beneficial, its effectiveness remains suboptimal due to the vertical position limitations that do not cover the entire building mass.

Based on the results of the comparison of the deviation values between the above levels, it can be seen that the first model, which uses a belt truss and outrigger system on floors 35-36 and 55-57, shows a maximum drift value of 31.224 mm in the X direction and 35.327 mm in the Y direction. These results indicate that the presence of the lateral force transfer system has made a significant contribution to reducing relative deformation between floors, particularly in the middle to upper sections of the building. However, since this system is only installed at two specific vertical points, deformation control is not uniformly distributed throughout the structure, leaving the possibility of high drift concentration on floors not directly served by the system. This indicates that while the belt truss and outrigger system has improved structural performance, its uneven distribution results in inconsistent drift control across all levels.

The following are the displacement curves in the X and Y directions in model 1 and the drift curves in the X and Y directions in model 1.

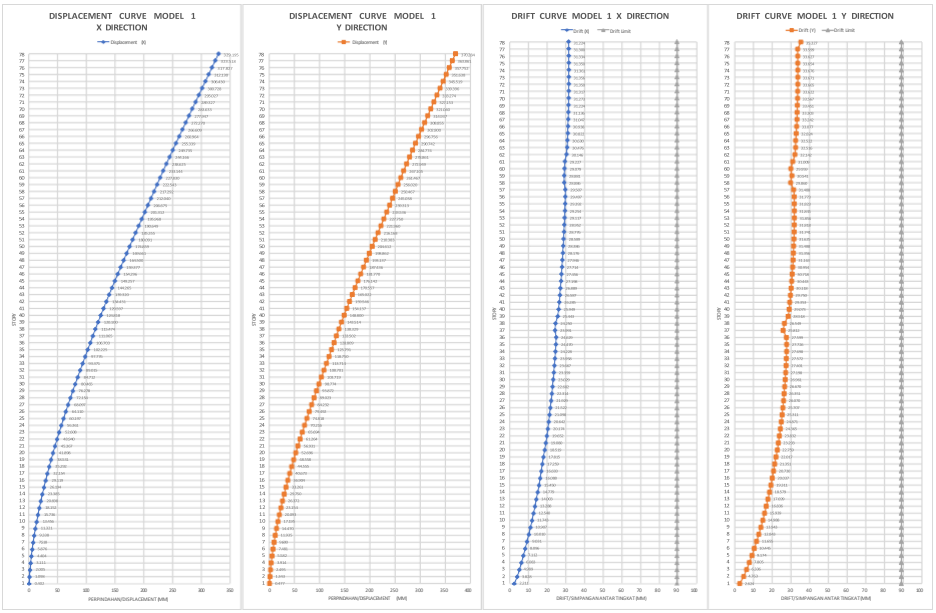

Figure 7. Displacement Curve and Drift Curve Model 1 in the X and Y Directions

Table 8: Displacement and Drift Values in Model 2

Story	Displacement		Elastic Drift		h_{sx}	Inelastic Drift		Drift Limit	Control
	δe_X	δe_Y	δe_X	δe_Y		Δ_X	Δ_Y	Δa	
	(mm)	(mm)	(mm)	(mm)	(mm)	(mm)	(mm)	(mm)	
78	331.526	381.038	5.749	6.599	4450	31.620	36.294	89.000	OK
77	325.777	374.439	5.763	6.343	4450	31.696	34.887	89.000	OK
76	320.014	368.096	5.768	6.348	4450	31.724	34.914	89.000	OK
75	314.246	361.748	5.771	6.355	4450	31.740	34.953	89.000	OK
74	308.475	355.393	5.773	6.361	4450	31.752	34.985	89.000	OK
73	302.702	349.032	5.774	6.365	4450	31.757	35.008	89.000	OK
72	296.928	342.667	5.772	6.369	4450	31.746	35.029	89.000	OK
71	291.156	336.298	5.769	6.370	4450	31.730	35.035	89.000	OK
70	285.387	329.928	5.763	6.369	4450	31.696	35.029	89.000	OK
69	279.624	323.559	5.755	6.360	4450	31.653	34.980	89.000	OK
68	273.869	317.199	5.741	6.346	4450	31.576	34.903	89.000	OK
67	268.128	310.853	5.728	6.349	4450	31.504	34.919	89.000	OK
66	262.400	304.504	5.714	6.339	4450	31.427	34.865	89.000	OK
65	256.686	298.165	5.696	6.321	4450	31.328	34.766	89.000	OK
64	250.990	291.844	5.669	6.294	4450	31.180	34.617	89.000	OK
63	245.321	285.550	5.648	6.312	4450	31.064	34.716	89.000	OK
62	239.673	279.238	5.608	6.270	4450	30.844	34.485	89.000	OK
61	234.065	272.968	5.582	6.232	4450	30.701	34.276	89.000	OK
60	228.483	266.736	5.556	6.207	4450	30.558	34.139	89.000	OK
59	222.927	260.529	5.528	6.179	4450	30.404	33.985	89.000	OK
58	217.399	254.350	5.500	6.162	4450	30.250	33.891	89.000	OK
57	211.899	248.188	5.469	6.138	4450	30.080	33.759	89.000	OK
56	206.430	242.050	5.438	6.110	4450	29.909	33.605	89.000	OK
55	200.992	235.940	5.405	6.078	4450	29.728	33.429	89.000	OK
54	195.587	229.862	5.370	6.046	4450	29.535	33.253	89.000	OK
53	190.217	223.816	5.334	6.023	4450	29.337	33.127	89.000	OK
52	184.883	217.793	5.297	5.991	4450	29.134	32.951	89.000	OK
51	179.586	211.802	5.259	5.958	4450	28.925	32.769	89.000	OK
50	174.327	205.844	5.219	5.923	4450	28.705	32.577	89.000	OK
49	169.108	199.921	5.178	5.885	4450	28.479	32.367	89.000	OK
48	163.930	194.036	5.136	5.851	4450	28.248	32.181	89.000	OK
47	158.794	188.185	5.093	5.813	4450	28.012	31.971	89.000	OK
46	153.701	182.372	5.048	5.772	4450	27.764	31.746	89.000	OK
45	148.653	176.600	5.003	5.731	4450	27.516	31.521	89.000	OK
44	143.650	170.869	4.955	5.687	4450	27.253	31.279	89.000	OK
43	138.695	165.182	4.902	5.637	4450	26.961	31.004	89.000	OK
42	133.793	159.545	4.850	5.587	4450	26.675	30.728	89.000	OK

Story	Displacement		Elastic Drift		h_{sx}	Inelastic Drift		Drift Limit	Control
	δe_X	δe_Y	δe_X	δe_Y		Δ_X	Δ_Y	Δa	
	(mm)	(mm)	(mm)	(mm)	(mm)	(mm)	(mm)	(mm)	
41	128.943	153.958	4.800	5.532	4450	26.400	30.426	89.000	OK
40	124.143	148.426	4.745	5.497	4450	26.098	30.233	89.000	OK
39	119.398	142.929	4.674	5.435	4450	25.707	29.893	89.000	OK
38	114.724	137.494	4.622	5.365	4450	25.421	29.508	89.000	OK
37	110.102	132.129	4.570	5.312	4450	25.135	29.216	89.000	OK
36	105.532	126.817	4.517	5.252	4450	24.844	28.886	89.000	OK
35	101.015	121.565	4.460	5.193	4450	24.530	28.562	89.000	OK
34	96.555	116.372	4.404	5.144	4450	24.222	28.292	89.000	OK
33	92.151	111.228	4.344	5.084	4450	23.892	27.962	89.000	OK
32	87.807	106.144	4.284	5.021	4450	23.562	27.616	89.000	OK
31	83.523	101.123	4.220	4.956	4450	23.210	27.258	89.000	OK
30	79.303	96.167	4.153	4.887	4450	22.842	26.879	89.000	OK
29	75.150	91.280	4.086	4.811	4450	22.473	26.461	89.000	OK
28	71.064	86.469	4.013	4.733	4450	22.072	26.031	89.000	OK
27	67.051	81.736	3.940	4.665	4450	21.670	25.658	89.000	OK
26	63.111	77.071	3.863	4.584	4450	21.247	25.212	89.000	OK
25	59.248	72.487	3.782	4.498	4450	20.801	24.739	89.000	OK
24	55.466	67.989	3.699	4.409	4450	20.345	24.250	89.000	OK
23	51.767	63.580	3.611	4.309	4450	19.861	23.700	89.000	OK
22	48.156	59.271	3.516	4.204	4450	19.338	23.122	89.000	OK
21	44.640	55.067	3.412	4.104	4450	18.766	22.572	89.000	OK
20	41.228	50.963	3.311	4.005	4450	18.211	22.028	89.000	OK
19	37.917	46.958	3.184	3.870	4450	17.512	21.285	89.000	OK
18	34.733	43.088	3.085	3.751	4450	16.968	20.631	89.000	OK
17	31.648	39.337	2.982	3.639	4450	16.401	20.015	89.000	OK
16	28.666	35.698	2.876	3.515	4450	15.818	19.333	89.000	OK
15	25.790	32.183	2.761	3.387	4450	15.186	18.629	89.000	OK
14	23.029	28.796	2.641	3.260	4450	14.526	17.930	89.000	OK
13	20.388	25.536	2.504	3.106	4450	13.772	17.083	89.000	OK
12	17.884	22.430	2.377	2.954	4450	13.074	16.247	89.000	OK
11	15.507	19.476	2.242	2.800	4450	12.331	15.400	89.000	OK
10	13.265	16.676	2.103	2.633	4450	11.567	14.482	89.000	OK
9	11.162	14.043	1.953	2.452	4450	10.742	13.486	89.000	OK
8	9.209	11.591	1.794	2.260	4450	9.867	12.430	89.000	OK
7	7.415	9.331	1.618	2.049	4450	8.899	11.270	89.000	OK
6	5.797	7.282	1.449	1.840	4450	7.970	10.120	89.000	OK
5	4.348	5.442	1.275	1.618	4450	7.013	8.899	89.000	OK
4	3.073	3.824	1.091	1.381	4450	6.001	7.596	89.000	OK
3	1.982	2.443	0.895	1.123	4450	4.923	6.177	89.000	OK
2	1.087	1.320	0.688	0.848	4450	3.784	4.664	89.000	OK
1	0.399	0.472	0.399	0.472	4450	2.195	2.593	89.000	OK

Based on the output results from ETABS in modeling 2, the maximum displacement value on floor 78 was obtained at 331.526 mm in the X direction and 381.038 mm in the Y direction. Therefore, the calculation of the inter-story drift in modeling 2 with the placement of the existing belt truss and outrigger system obtained a maximum drift value on floor 78 (top story) caused by the seismic response spectrum in the X direction of 31.620 mm and in the Y direction of 36.294 mm.

Meanwhile, the second modeling, which does not apply the belt truss or outrigger system and relies solely on the corewall element as the primary lateral force-resisting system, shows that lateral displacement increases to 331.526 mm in the X direction and 381.038 mm in the Y direction. Although the difference in these values compared to the first model appears numerically insignificant, structurally, this increase confirms that the absence of the belt truss and outrigger systems prevents lateral forces from being optimally distributed to the perimeter columns, causing all lateral loads to concentrate on the corewall. This naturally results in greater structural deformation, particularly at the building's peak, and highlights the weakness of a structural system overly reliant on a single lateral force-bearing element.

In the second modeling, which does not involve the belt truss and outrigger systems at all, the drift values increase to 31.620 mm in the X direction and 36.294 mm in the Y direction, making it the model with the worst drift performance among the three. These values indicate that when there is no additional lateral force distribution system connecting the corewall to the perimeter columns, inter-story deformation becomes larger and more uncontrolled. This certainly has serious implications for the stability of non-structural elements such as partition walls, ceilings, and mechanical and electrical systems that are highly sensitive to changes in floor geometry. Thus, the absence of belt truss and outrigger systems in this scenario poses a greater risk of internal building damage, even when the main structure does not collapse.

The following are the displacement curves in the X and Y directions in model 2 and the drift curves in the X and Y directions in model 2.

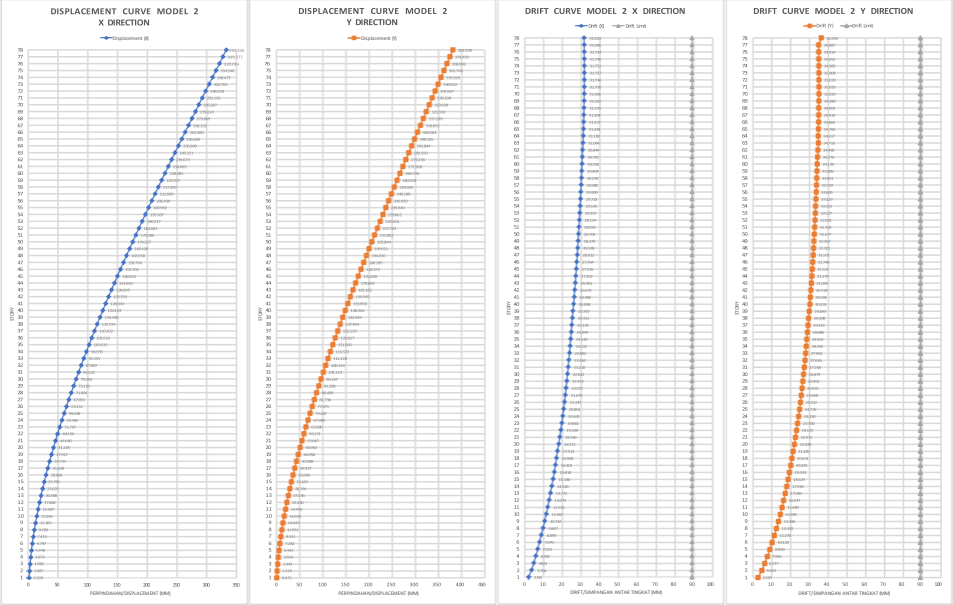

Figure 8. Displacement Curve and Drift Curve Model 2 in the X and Y Directions

Table 9: Displacement and Drift Values in Model 3

Story	Displacement		Elastic Drift		h_{sx}	Inelastic Drift		Drift Limit	Control
	δe_X	δe_Y	δe_X	δe_Y		Δ_X	Δ_Y	Δa	
	(mm)	(mm)	(mm)	(mm)	(mm)	(mm)	(mm)	(mm)	
78	324.286	359.281	5.652	6.398	4450	31.086	35.189	89.000	OK
77	318.634	352.883	5.666	6.090	4450	31.163	33.495	89.000	OK
76	312.968	346.793	5.671	6.096	4450	31.191	33.528	89.000	OK
75	307.297	340.697	5.675	6.103	4450	31.213	33.567	89.000	OK
74	301.622	334.594	5.677	6.107	4450	31.224	33.588	89.000	OK
73	295.945	328.487	5.678	6.110	4450	31.229	33.605	89.000	OK
72	290.267	322.377	5.676	6.109	4450	31.218	33.600	89.000	OK
71	284.591	316.268	5.672	6.106	4450	31.196	33.583	89.000	OK
70	278.919	310.162	5.664	6.098	4450	31.152	33.539	89.000	OK
69	273.255	304.064	5.656	6.079	4450	31.108	33.435	89.000	OK
68	267.599	297.985	5.640	6.057	4450	31.020	33.314	89.000	OK
67	261.959	291.928	5.626	6.050	4450	30.943	33.275	89.000	OK
66	256.333	285.878	5.607	6.024	4450	30.839	33.132	89.000	OK
65	250.726	279.854	5.587	5.983	4450	30.728	32.907	89.000	OK
64	245.139	273.871	5.555	5.935	4450	30.553	32.643	89.000	OK
63	239.584	267.936	5.526	5.939	4450	30.393	32.664	89.000	OK
62	234.058	261.997	5.470	5.875	4450	30.085	32.313	89.000	OK
61	228.588	256.122	5.291	5.634	4450	29.101	30.987	89.000	OK
60	223.297	250.488	5.276	5.451	4450	29.018	29.981	89.000	OK
59	218.021	245.037	5.395	5.762	4450	29.672	31.691	89.000	OK
58	212.626	239.275	5.392	5.809	4450	29.656	31.950	89.000	OK
57	207.234	233.466	5.370	5.811	4450	29.535	31.961	89.000	OK
56	201.864	227.655	5.345	5.806	4450	29.398	31.933	89.000	OK
55	196.519	221.849	5.318	5.783	4450	29.249	31.806	89.000	OK
54	191.201	216.066	5.286	5.764	4450	29.073	31.702	89.000	OK
53	185.915	210.302	5.254	5.750	4450	28.897	31.625	89.000	OK
52	180.661	204.552	5.218	5.723	4450	28.699	31.476	89.000	OK
51	175.443	198.829	5.182	5.692	4450	28.501	31.306	89.000	OK
50	170.261	193.137	5.142	5.654	4450	28.281	31.097	89.000	OK
49	165.119	187.483	5.100	5.612	4450	28.050	30.866	89.000	OK
48	160.019	181.871	5.057	5.571	4450	27.814	30.641	89.000	OK
47	154.962	176.300	5.012	5.522	4450	27.566	30.371	89.000	OK
46	149.950	170.778	4.963	5.467	4450	27.297	30.068	89.000	OK
45	144.987	165.311	4.913	5.405	4450	27.021	29.728	89.000	OK
44	140.074	159.906	4.860	5.338	4450	26.730	29.359	89.000	OK
43	135.214	154.568	4.797	5.265	4450	26.384	28.958	89.000	OK
42	130.417	149.303	4.723	5.174	4450	25.977	28.457	89.000	OK

Story	Displacement		Elastic Drift		h_{sx}	Inelastic Drift		Drift Limit	Control
	δe_X	δe_Y	δe_X	δe_Y		Δ_X	Δ_Y	Δa	
	(mm)	(mm)	(mm)	(mm)	(mm)	(mm)	(mm)	(mm)	
41	125.694	144.129	4.494	4.825	4450	24.717	26.537	89.000	OK
40	121.200	139.304	4.446	4.707	4450	24.453	25.889	89.000	OK
39	116.754	134.597	4.549	5.014	4450	25.020	27.577	89.000	OK
38	112.205	129.583	4.523	5.011	4450	24.877	27.561	89.000	OK
37	107.682	124.572	4.479	4.990	4450	24.635	27.445	89.000	OK
36	103.203	119.582	4.435	4.955	4450	24.393	27.253	89.000	OK
35	98.768	114.627	4.382	4.914	4450	24.101	27.027	89.000	OK
34	94.386	109.713	4.330	4.883	4450	23.815	26.857	89.000	OK
33	90.056	104.830	4.274	4.836	4450	23.507	26.598	89.000	OK
32	85.782	99.994	4.215	4.783	4450	23.183	26.307	89.000	OK
31	81.567	95.211	4.152	4.724	4450	22.836	25.982	89.000	OK
30	77.415	90.487	4.087	4.660	4450	22.479	25.630	89.000	OK
29	73.328	85.827	4.018	4.583	4450	22.099	25.207	89.000	OK
28	69.310	81.244	3.945	4.503	4450	21.698	24.767	89.000	OK
27	65.365	76.741	3.869	4.429	4450	21.280	24.360	89.000	OK
26	61.496	72.312	3.789	4.339	4450	20.840	23.865	89.000	OK
25	57.707	67.973	3.705	4.238	4450	20.378	23.309	89.000	OK
24	54.002	63.735	3.616	4.132	4450	19.888	22.726	89.000	OK
23	50.386	59.603	3.520	4.011	4450	19.360	22.061	89.000	OK
22	46.866	55.592	3.403	3.860	4450	18.717	21.230	89.000	OK
21	43.463	51.732	3.148	3.468	4450	17.314	19.074	89.000	OK
20	40.315	48.264	3.051	3.345	4450	16.781	18.398	89.000	OK
19	37.264	44.919	3.077	3.538	4450	16.924	19.459	89.000	OK
18	34.187	41.381	3.004	3.489	4450	16.522	19.190	89.000	OK
17	31.183	37.892	2.913	3.411	4450	16.022	18.761	89.000	OK
16	28.270	34.481	2.813	3.317	4450	15.472	18.244	89.000	OK
15	25.457	31.164	2.707	3.215	4450	14.889	17.683	89.000	OK
14	22.750	27.949	2.593	3.109	4450	14.262	17.100	89.000	OK
13	20.157	24.840	2.461	2.975	4450	13.536	16.363	89.000	OK
12	17.696	21.865	2.339	2.842	4450	12.865	15.631	89.000	OK
11	15.357	19.023	2.210	2.702	4450	12.155	14.861	89.000	OK
10	13.147	16.321	2.073	2.551	4450	11.402	14.031	89.000	OK
9	11.074	13.770	1.929	2.382	4450	10.610	13.101	89.000	OK
8	9.145	11.388	1.773	2.204	4450	9.752	12.122	89.000	OK
7	7.372	9.184	1.602	2.006	4450	8.811	11.033	89.000	OK
6	5.770	7.178	1.437	1.805	4450	7.904	9.928	89.000	OK
5	4.333	5.373	1.267	1.592	4450	6.969	8.756	89.000	OK
4	3.066	3.781	1.085	1.361	4450	5.968	7.486	89.000	OK
3	1.981	2.420	0.893	1.110	4450	4.912	6.105	89.000	OK
2	1.088	1.310	0.688	0.842	4450	3.784	4.631	89.000	OK
1	0.400	0.468	0.400	0.468	4450	2.200	2.574	89.000	OK

Based on the output results from ETABS in modeling 3, the maximum displacement value on floor 78 was obtained at 324.286 mm in the X direction and 359.281 mm in the Y direction. Therefore, the calculation of the inter-story drift in modeling 3 with the placement of the existing belt truss and outrigger system obtained a maximum drift value on floor 78 (top story) caused by the seismic response spectrum in the X direction of 31.086 mm and in the Y direction of 35.189 mm.

Unlike the previous two models, the third model, which uses a distributed approach for the belt truss and outrigger systems at three main vertical points—namely floors 18–20, 37–39, and 56–57—shows the most effective performance in resisting lateral displacement. The analysis results show a maximum displacement value of 324.286 mm in the X direction and 359.281 mm in the Y direction. This consistent and significant reduction in values is concrete evidence that the strategy of distributing the belt truss and outrigger systems can enhance the building's lateral stiffness comprehensively, not just in specific zones. By incorporating this system at multiple levels, the structure gains additional vertical resistance, so that lateral forces caused by earthquakes are not confined to one or two locations but are distributed to various load-bearing points, resulting in more controlled global deformation. Thus, it can be concluded that the third modeling provides the most ideal implementation of the system for significantly reducing displacement values through more even and efficient stiffness distribution.

Conversely, the third modeling once again demonstrates the best performance in controlling drift values, with maximum results of 31.086 mm in the X direction and 35.189 mm in the Y direction. This serves as strong evidence that the strategy of gradually and evenly distributing the belt truss and outrigger systems can more effectively mitigate local deformation compared to other approaches. By connecting the corewall and perimeter columns at three relatively evenly spaced levels from bottom to top, this system forms a more continuous and layered lateral restraint path, thereby minimizing differences in deflection between levels as early as possible from

the bottom of the structure. This not only reduces the risk of non-structural damage but also provides a higher sense of safety and comfort for building occupants during an earthquake. Therefore, the third modeling approach can be considered the most effective method for controlling local deformation in supertall buildings.

The following are the displacement curves in the X and Y directions in model 3 and the drift curves in the X and Y directions in model 3.

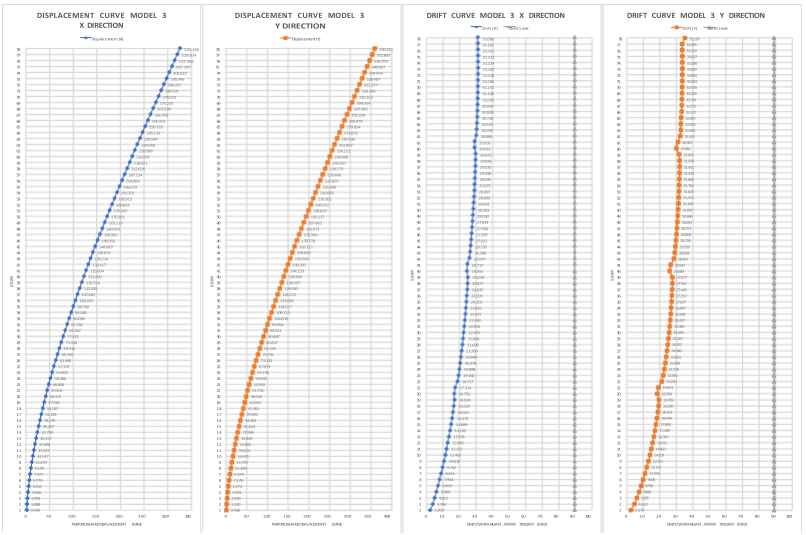

Figure 9. Displacement Curve and Drift Curve Model 3 in the X and Y Directions

When determining the performance level of a structure, the maximum total deflection and maximum inelastic deflection values are required. The following formula is used to calculate these values.

$$\text{Maximum Total Drift} = D_t / H_{tot} \quad (2)$$

$$\text{Maximum Inelastic Drift} = (D_t - D_1) / H_{tot} \quad (3)$$

Where:
D_t = Maximum displacement of the structure on the top floor (m)
D_1 = Displacement at the first yield condition or first floor (m)
H_{tot} = Total height of the structure (m)

Table 10: Performance Level of Model Structures 1, 2, and 3

Drift	Model 1		Model 2		Model 3	
	X Direction	Y Direction	X Direction	Y Direction	X Direction	Y Direction
Maximum Total Drift	0.000948	0.001067	0.000955	0.001098	0.000934	0.001035
Maximum Inelastic Drift	0.000947	0.001065	0.000954	0.001096	0.000933	0.001034
Structural Performance Level	**IO**	**IO**	**IO**	**IO**	**IO**	**IO**

Based on the evaluation and calculations performed on three supertall building models, the structure was found to meet the Immediate Occupancy (IO) performance criteria as defined by ATC-40. This means that the structure is still capable of maintaining its stability and capacity to withstand gravitational loads and seismic loads without suffering significant damage to its main structural elements. The lateral load-bearing system, including the frame and shear walls, remains fully functional without showing signs of local collapse or plastic failure beyond the elastic limit. Additionally, non-structural elements only experienced minor damage that does not affect the building's functionality and safety. As a result, the building can be immediately reused after an earthquake without requiring significant structural repairs, ensuring that building operations continue with minimal disruption and occupant safety risks remain controlled. This performance level generally reflects the structure's readiness to maintain its residential or operational functions as soon as possible after a seismic event occurs.

4. CONCLUSIONS

Based on the results of a series of analysis, calculations, and in-depth studies conducted through modeling, loading, and layered evaluation stages, this research produced several important conclusions that can be used as a reference for understanding the performance of supertall buildings using the belt truss and outrigger system approach. These conclusions are systematically and structurally formulated to provide a comprehensive overview of the role, advantages, and potential improvements of the structural system in such tall buildings, as detailed below.

Based on the evaluation results obtained from the three modeling scenarios examined at the 78th floor as the top floor, Modeling 1, which represents the existing conditions with a belt truss and outrigger system on floors 35–36

and 55–57, shows displacement values of 329.195 mm in the X direction and 342.202 mm in the Y direction. Modeling 2, which does not use the belt truss and outrigger system, produces the largest displacement values, namely 331.526 mm in the X direction and 347.076 mm in the Y direction. Meanwhile, Model 3, which applied the belt truss and outrigger system in three strategic zones on floors 18–20, 37–39, and 56–57, showed the best performance with the smallest displacement values, namely 324.286 mm in the X direction and 336.759 mm in the Y direction.

Regarding the inter-story drift for the three models, as observed from the 78th floor as the top floor, Model 1 recorded a drift value of 31.224 mm in the X direction and 33.076 mm in the Y direction. Model 2 again showed the largest drift values, namely 31.620 mm in the X direction and 33.698 mm in the Y direction. Meanwhile, Model 3 achieved the smallest drift values, namely 31.086 mm in the X direction and 32.495 mm in the Y direction.

Performance evaluation of the structure based on ATC-40 guidelines indicates that all three models are at the Immediate Occupancy (IO) level. This level indicates that the building can still be used immediately after an earthquake with minimal structural and non-structural damage. This means that the primary functions of the building remain operational without requiring significant repairs, and the safety of occupants is maintained.

Based on the results of analysis and evaluation, it is evident that modeling performance 1 and 3 consistently show lower displacement and drift values, particularly on the 78th floor, which is the most critical point and the top floor. This indicates that the belt truss and outrigger systems are highly effective in enhancing structural stiffness and resisting lateral deformation caused by earthquakes. Therefore, the application of this system should no longer be considered an optional addition but rather a primary strategy in the design of supertall buildings in seismic regions such as Jakarta.

The poor performance demonstrated by Model 2 in terms of displacement, drift, and design verification results indicates that a corewall system without additional lateral support is inadequate for structures of extreme height. Especially since the largest displacement and drift values occur on the 78th floor, indicating that the top floor is most vulnerable to structural damage if not equipped with a lateral restraint system. This underscores the importance of considering belt truss and outrigger systems as primary structural elements rather than mere design supplements.

The performance-based evaluation approach outlined in ATC-40 has proven capable of comprehensively describing structural conditions, not only in terms of strength but also post-earthquake functionality. All three models indeed indicate an Immediate Occupancy level. Considering that the top floor tends to experience maximum deformation, the ATC-40-based evaluation is highly relevant for assessing the structural integrity of supertall buildings in earthquake scenarios and should be adopted as the evaluation standard in professional practice.

ACKNOWLEDGMENT

The author would like to thank Drs. Budi Kudwadi, M.T. and Ben Novarro Batubara, M.T. as supervisors for their guidance and input during this research process. Appreciation is also extended to the owner of the supertall building, particularly the Structural Engineering Manager and Chief Resident Engineer, for the technical data and administrative support provided. This research would not have been possible without the role and cooperation of all these parties.

REFERENCES

Elnashai AS, Di Sarno L. Fundamentals of earthquake engineering. Chichester (UK): John Wiley & Sons; 2008. 356p.
Shivakumar GS. High-rise buildings: Challenges and technical innovations. Singapore: Springer; 2023. 216p.
Alhaddad W. The influence of fin systems and truss frames on the seismic performance of high-rise buildings. IOP Conference Series: Materials Science and Engineering. 2020;949(1):012026. https://doi.org/10.1088/1757-899X/949/1/012026
Smith BS, Coull A. High-rise building structures: Analysis and design. New York: John Wiley & Sons; 1991. 537p.
Hasdanita A, Harahap TR, Yani A. Evaluation of the performance of multi-story building structures against earthquake forces using the spectrum response analysis method. Journal of Civil Engineering and Planning. 2023;25(2):95-102.
Applied Technology Council. Seismic evaluation and retrofit of concrete buildings. Redwood City (CA): Applied Technology Council; 1996. Report Number: ATC-40.
National Standardization Agency. SNI 1726:2019 Procedures for earthquake resistance design for building and non-building structures. Jakarta: BSN; 2019. 215p.

National Standardization Agency. SNI 1727:2020 Minimum loads for the design of buildings and other structures. Jakarta: BSN; 2020. 143p.
Chopra AK. Dynamics of structures: Theory and applications to earthquake engineering. 5th ed. New York: Pearson; 2020. 944p.
Computers and Structures, Inc. ETABS: Integrated building design software – User's manual. Berkeley (CA): Computers and Structures, Inc.; 2020. 650p.